

# Synthesis and Radiation Response Properties of Tm-activated Na<sub>2</sub>O–ZnO–TeO<sub>2</sub>–B<sub>2</sub>O<sub>3</sub> Glasses

Kai Okazaki,\* Daisuke Nakauchi, Akihiro Nishikawa, Takumi Kato,  
Noriaki Kawaguchi, and Takayuki Yanagida

Division of Materials Science, Nara Institute of Science and Technology (NAIST),  
8916-5 Takayama-Cho Ikoma, Nara 630-0192, Japan

(Received October 30, 2023; accepted January 18, 2024)

**Keywords:** phosphor, radiation measurement, scintillation, borate glass

Na<sub>2</sub>O–ZnO–TeO<sub>2</sub>–B<sub>2</sub>O<sub>3</sub> (NZTB) glasses doped with Tm (0.1, 0.5, 1, and 2%) were synthesized by a conventional melt quenching technique, and their photoluminescence and scintillation properties were investigated. Some emission peaks due to the electronic transitions of Tm<sup>3+</sup> appeared upon ultraviolet light and X-ray irradiation. Decay times were valid as the 4f–4f transitions of Tm<sup>3+</sup>. A 1% Tm-doped NZTB glass showed a full absorption peak under <sup>241</sup>Am  $\alpha$ -ray irradiation, and the light yield was estimated to be 51 photons/5.5 MeV- $\alpha$  when the peak channel was compared with a photoabsorption peak of <sup>137</sup>Cs  $\gamma$ -rays measured with a Ce-doped Gd<sub>2</sub>SiO<sub>5</sub> sample.

## 1. Introduction

Scintillators are luminescence materials that promptly convert high-energy ionizing radiation into low-energy photons after absorbing the energy.<sup>(1–3)</sup> They have been used in many fields, for example, medical imaging,<sup>(4)</sup> security inspection,<sup>(5)</sup> environmental measurement,<sup>(6)</sup> and resource exploration.<sup>(7)</sup> The following properties are generally important for scintillators: high light yield (*LY*), fast decay, low afterglow, and mechanical and chemical stabilities. There are no scintillators satisfying all the above properties. However, the required properties vary in applications; therefore, suitable scintillators are chosen on the basis of their physical and chemical properties. From the perspective of material form, many types of material have been applied, for instance, crystals,<sup>(8–11)</sup> ceramics,<sup>(12–14)</sup> liquids,<sup>(15–17)</sup> and glasses.<sup>(18–22)</sup> Glasses are an attractive form owing to their low cost, ease of formability, high mechanical strength, and high freedom in composition selection. In particular, Ce-doped lithium silicate glasses have been intensively studied for thermal neutron detection,<sup>(19,23–25)</sup> and GS20, which shows the *LY* of 6000 photons/neutron<sup>(26)</sup> with no hygroscopicity and low density, is a commercial glass scintillator. For thermal neutron detection, a <sup>3</sup>He gas counter is mainly applied by using <sup>3</sup>He(n, p)<sup>3</sup>H reactions,<sup>(27)</sup> however, alternative detectors are extensively studied because of the limitation of <sup>3</sup>He resources.<sup>(28)</sup>

---

\*Corresponding author: e-mail: [okazaki.kai.of0@ms.naist.jp](mailto:okazaki.kai.of0@ms.naist.jp)  
<https://doi.org/10.18494/SAM4753>

Borate glasses to be used for thermal neutron detection in addition to Li-containing glasses have also received attention because  $^{10}\text{B}$  has a larger thermal neutron capture cross section (3840 barn) than  $^6\text{Li}$  (940 barn).<sup>(29)</sup> Some compositions with borate have shown response to neutrons or  $\alpha$ -rays;<sup>(30–33)</sup> however, there are no commercial ones. In this study,  $\text{Na}_2\text{O}$ – $\text{ZnO}$ – $\text{TeO}_2$ – $\text{B}_2\text{O}_3$  (NZTB) glasses were developed. The prepared glasses have almost the same effective atomic number (29) as GS20 (26),<sup>(34)</sup> and the relatively low value is an advantage for distinguishing signals of neutrons from those of  $\gamma$ -rays.  $\text{TeO}_2$  improves thermal strength, chemical stability, and light output when combined with  $\text{B}_2\text{O}_3$ .<sup>(35,36)</sup> Borate glasses generally show high hygroscopicity; therefore,  $\text{Na}_2\text{O}$  was added as a modifier.<sup>(37)</sup> Moreover, alkali-metal-oxide-containing  $\text{ZnO}$ – $\text{TeO}_2$ – $\text{B}_2\text{O}_3$  glasses were discovered to show good transparency in visible ranges.<sup>(38,39)</sup> This optical characteristic is suitable for the host material for scintillators with luminescence centers. Some rare-earth ions act as luminescence centers.<sup>(40–42)</sup> Tm exhibits sharp emissions in visible–infrared regions due to electric dipole-forbidden transitions between 4f orbitals.<sup>(43–45)</sup> The main peaks appear in the 300–500 nm range,<sup>(46–49)</sup> which matches the high wavelength sensitivity regions of conventional photodetectors such as photomultiplier tubes and Si photodiodes. Here, we fabricated NZTB glasses doped with different Tm concentrations, and investigated their optical and scintillation properties.

## 2. Materials and Methods

$25\text{Na}_2\text{O}$ – $20\text{ZnO}$ – $5\text{TeO}_2$ – $50\text{B}_2\text{O}_3$  glasses doped with Tm (0, 0.1, 0.5, 1, and 2 mol%) were synthesized by the melt quenching method. First,  $\text{Tm}_2\text{O}_3$  (4N),  $\text{Na}_2\text{CO}_3$  (4N),  $\text{ZnO}$  (4N),  $\text{TeO}_2$  (4N), and  $\text{B}_2\text{O}_3$  (5N) powders were homogeneously mixed with an agate mortar. Then, they were transferred to an alumina crucible and melted at 900 °C for 1 h. After that, the melt was flowed onto a preheated stainless-steel plate to quench. The obtained samples were annealed at 300 °C for 1 h to remove thermal and mechanical strains. The annealing temperature was determined by measuring the glass transition temperature ( $T_g$ ) of the undoped sample with a TG-DTA system (Hitachi High-Tech Corporation, STA7200).

The densities of the prepared samples were measured using an analytical balance (A&D Company, GR-120). Ultrapure water (Fujifilm Wako) was used in the measurement. Powder X-ray diffraction (XRD) patterns were determined using a diffractometer (Rigaku, MiniFlex600). Diffuse transmission spectra were measured with a spectrometer (Shimadzu, SolidSpec-3700). The photoluminescence (PL) excitation and emission spectra, PL quantum yields (QYs), and PL decay curves were calculated using a Quantaaurus-QY (Hamamatsu, C11347) and a Quantaaurus- $\tau$  (Hamamatsu, C11367). As radiation response properties, X-ray-induced scintillation spectra, X-ray-induced scintillation decay curves, and pulse height spectra of  $^{241}\text{Am}$   $\alpha$ -rays (5.5 MeV) were tested with our original setups.<sup>(50,51)</sup>

### 3. Results and Discussion

Figure 1 shows the photograph and densities of the prepared samples. The surfaces were polished for the following PL and scintillation measurements. All the samples appeared transparent and colorless under room light. The  $T_g$  of the undoped sample was 500 °C. The densities were changed in the range of 2.4–2.7 g/cm<sup>3</sup> with respect to the Tm concentration. As the dopant concentration increased, the densities increased owing to the molecular mass of Tm<sub>2</sub>O<sub>3</sub> being larger than that of the compounds composing the host. The values were comparable to that of GS20 (2.5 g/cm<sup>3</sup>).<sup>(26)</sup> Figure 2 shows the XRD patterns of the samples. Some parts of the glasses not used in the PL and scintillation measurements were crushed into powders, and XRD measurements were conducted. All the samples showed only halo peaks; hence, the samples had no periodical structures and formed glass phases.

Figure 3 shows the diffuse transmission spectra of NZTB glasses. The transmittance was 80–95% in the 350–850 nm range. Absorption peaks due to the electronic transitions of Tm<sup>3+</sup><sup>(52,53)</sup> were clearly observed at 350, 470, 680, and 790 nm in the 1 and 2% Tm-doped samples. Absorption edges were confirmed at 260–280 nm. They were slightly shifted to low-energy regions as the dopant concentration increased. As the Tm concentration increased, the peaks were shifted to low-energy regions. Figure 4 shows the PL excitation and emission spectra of the undoped and 0.5% Tm-doped NZTB glasses. Although the undoped sample did not show any emissions, the Tm-doped sample showed several emissions at 450, 480, 650, and 750 nm under excitation at 360 nm. These emissions were respectively considered to be derived from the <sup>1</sup>D<sub>2</sub>–<sup>3</sup>F<sub>4</sub>, <sup>1</sup>G<sub>4</sub>–<sup>3</sup>H<sub>6</sub>, <sup>1</sup>G<sub>4</sub>–<sup>3</sup>F<sub>4</sub>, and <sup>1</sup>D<sub>2</sub>–<sup>3</sup>F<sub>3</sub> transitions of Tm<sup>3+</sup>.<sup>(54,55)</sup> The QYs of the 0.1, 0.5, 1, and 2% Tm-doped samples were respectively 4.3, 8.6, 7.2, and 3.5% when monitored at 400–800 nm upon excitation at 360 nm. Figure 5 shows the PL decay curves of the Tm-doped samples. The

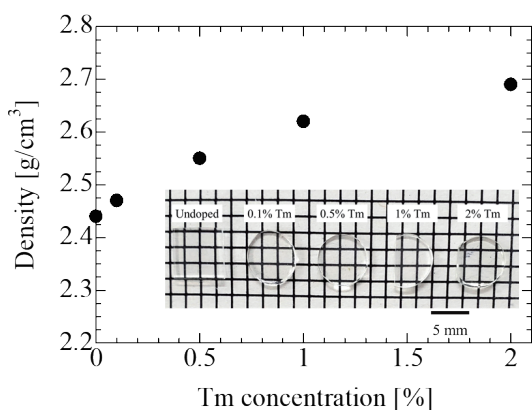


Fig. 1. Photograph (inset) and densities of NZTB glasses.

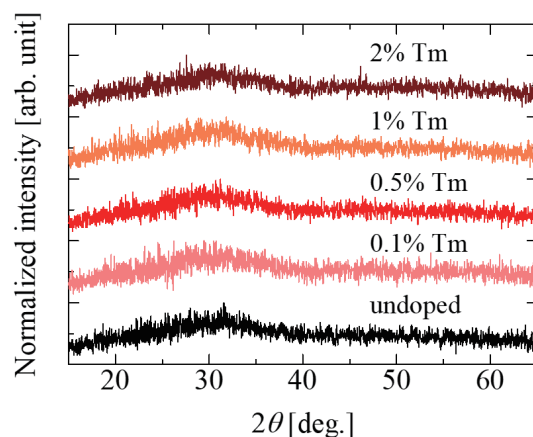


Fig. 2. (Color online) XRD patterns of NZTB glasses.

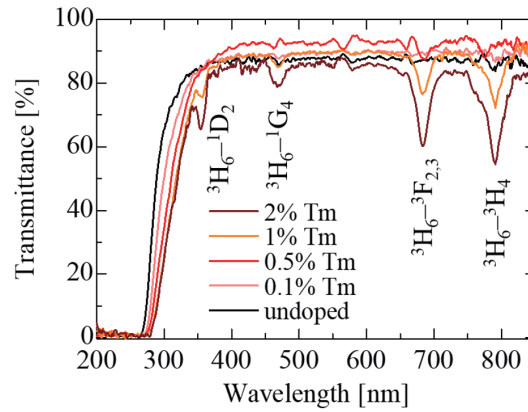


Fig. 3. (Color online) Diffuse transmission spectra of NZTB glasses.

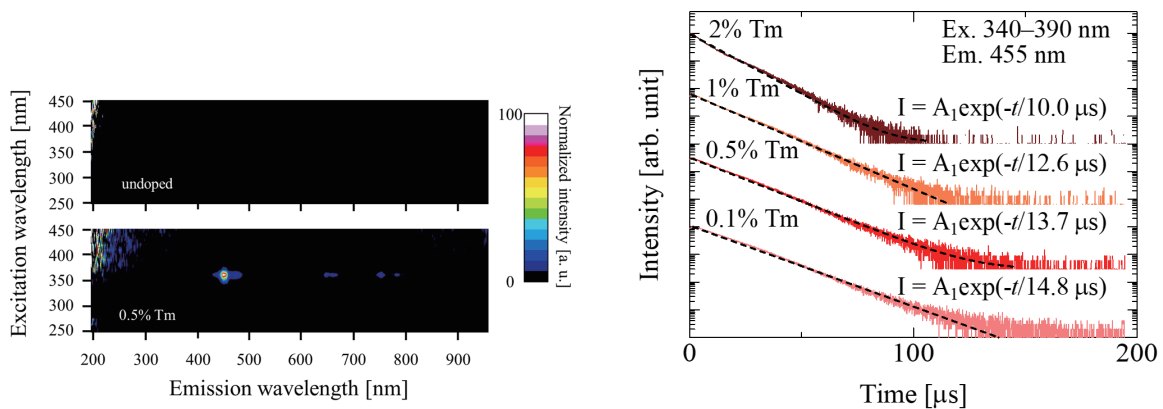


Fig. 4. (Color online) PL excitation and emission spectra of undoped and 0.5% Tm-doped NZTB glasses. Color scales indicate the intensities, where white and black indicate high and low intensities, respectively.

Fig. 5. (Color online) PL decay (solid) and fitting (dashed) curves of Tm-doped NZTB glasses. Excitation and monitored wavelengths were 340–390 nm and 455 nm, respectively.

obtained curves matched with an approximation by a single exponential decay function. The decay times of the 0.1, 0.5, 1, and 2% Tm-doped samples were obtained to be 14.8, 13.7, 12.6, and 10.0  $\mu\text{s}$ , respectively. From the above decay times and  $QY$ s, radiative ( $k_f$ ) and nonradiative ( $k_{nr}$ ) transition rates were estimated and are shown in Table 1. In the estimation, the following equations were applied:  $k_f = QY/\tau$  and  $k_{nr} = (1 - QY)/\tau$ . Here, the PL decay time was denoted as  $\tau$ .  $k_f$  decreased as the Tm concentration increased from 0.5 to 1%. The tendency can be described as concentration quenching that occurred at 1% Tm doping.

Figure 6 shows the X-ray-induced scintillation spectra of the NZTB glasses. Sharp emission peaks were observed at 350, 360, 450, and 480 nm. Similar scintillation peaks were observed in other Tm-doped materials;<sup>(56,57)</sup> hence, they were considered to be attributed to the 4f–4f transitions of  $\text{Tm}^{3+}$ . Figure 7 shows the X-ray-induced scintillation decay curves of the Tm-doped samples. All the curves were approximated by a single exponential function when the instrumental response function (IRF) was deconvoluted. The decay times were obtained to be

Table 1  
Summary of PL characteristics of Tm-doped NZTB glasses.

Samples	$QYs$ (%)	Decay times ( $\mu s$ )	$k_f$ ( $s^{-1}$ )	$k_{nr}$ ( $s^{-1}$ )
0.1% Tm	4.3	14.8	$2.9 \times 10^3$	$6.5 \times 10^4$
0.5% Tm	8.6	13.7	$6.3 \times 10^3$	$6.7 \times 10^4$
1% Tm	7.2	12.6	$5.8 \times 10^3$	$7.4 \times 10^4$
2% Tm	3.5	10.0	$3.5 \times 10^3$	$9.7 \times 10^4$

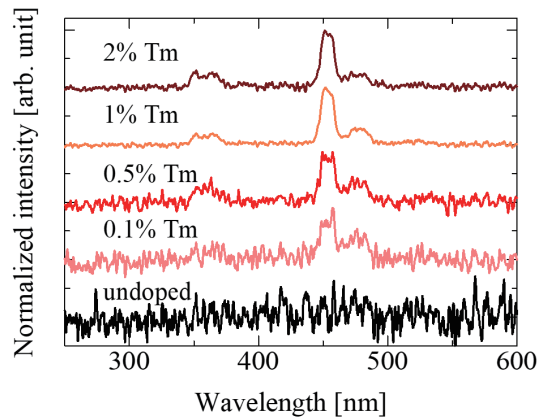


Fig. 6. (Color online) X-ray-induced scintillation spectra of NZTB glasses.

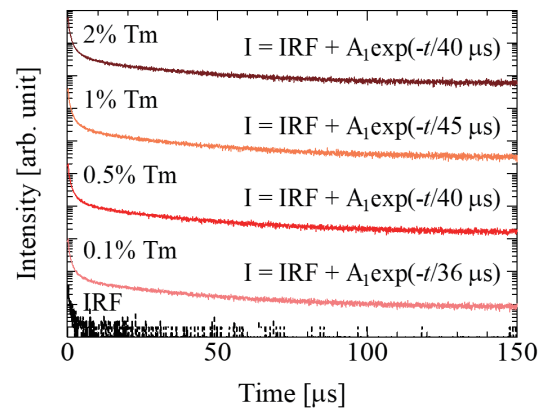


Fig. 7. (Color online) X-ray-induced scintillation decay curves of Tm-doped NZTB glasses.

30–50  $\mu s$ , which were close to the reported scintillation decay times of other Tm-doped materials.<sup>(48,57–59)</sup> Therefore, they originated from the 4f–4f transitions of  $Tm^{3+}$ . When compared with the PL decay times, they became much longer because of the conversion and transportation processes of scintillation in addition to the direct excitation and emission processes.<sup>(60)</sup>

Figure 8 shows the pulse height spectrum of  $^{241}Am$   $\alpha$ -rays (5.5 MeV) measured using the 1% Tm-doped NZTB glass. The spectrum of  $^{137}Cs$   $\gamma$ -rays (0.662 MeV) measured using a Ce-doped  $Gd_2SiO_5$  sample (GSO, 8000 photons/MeV) was also displayed as a reference for calculating the  $LY$  of a prepared sample. A full absorption peak appeared only in the 1% Tm-doped sample, whereas this peak was unclear in the spectra. The rest of the prepared samples did not show full absorption peaks owing to their low  $LY$ s. From Robbins' model,<sup>(61)</sup>  $LY$  is considered directly proportional to  $QY$ , but inversely proportion to bandgap energy ( $E_g$ ). The  $QY$  of the 0.5% Tm-doped sample was higher than that of the 1% Tm-doped sample; however, the 0.5% sample did not show a full absorption peak. This would be due to the difference in  $E_g$ : a high concentration of Tm doping would broaden the impurity bands and tails would reduce  $E_g$ .<sup>(62)</sup> This tendency was confirmed in the diffuse transmission spectra shown in Fig. 3. Therefore, the  $LY$  of the 1% Tm-doped sample would become higher than that of the 0.5% Tm-doped sample and the full absorption peak would appear. By comparing the channel of a full absorption peak (230 ch) with a photoabsorption peak channel of the reference (23750 ch), which was taking the difference in gain into account, the  $LY$  of the 1% Tm-doped glass was estimated to be 51 photons/5.5 MeV- $\alpha$ .

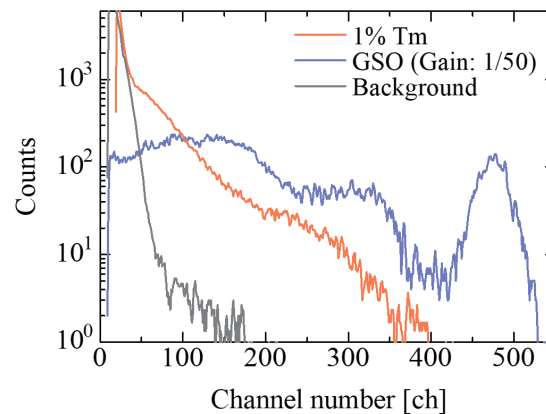


Fig. 8. (Color online) Pulse height spectra of  $^{241}\text{Am}$   $\alpha$ -rays (5.5 MeV) measured with 1% Tm-doped NZTB glass and  $^{137}\text{Cs}$   $\gamma$ -rays (0.662 MeV) measured using GSO. Background response was measured without samples.

#### 4. Conclusions

NZTB glasses doped with Tm (0.1, 0.5, 1, and 2%) were fabricated by a conventional melt quenching method, and their physical, PL, and scintillation properties were studied. The prepared samples had halo peaks and no sharp diffraction patterns. Their densities were 2.4–2.7  $\text{g}/\text{cm}^3$ , which were comparable to that of GS20. Under the irradiation of both ultraviolet light and X-rays, some emission peaks appeared in visible regions, and they originated from the 4f–4f transitions of  $\text{Tm}^{3+}$ . Although the prepared samples could not detect thermal neutrons, they showed signals under  $^{241}\text{Am}$   $\alpha$ -ray irradiation (5.5 MeV). The  $LY$  of the 1% Tm-doped sample was estimated to be 51 photons/5.5 MeV- $\alpha$ . Therefore, the result revealed that the glass with a composition of NZTB had a potential for thermal neutron detection because neutrons were detected through the observation of the  $\alpha$ -rays generated by neutron capture reactions. There is still huge room for research on NZTB glass scintillators because the molar ratio of host compositions, the optimum dopants, and their concentrations have not been investigated. By considering them, the  $QY$ ,  $LY$ , and capability of neutron detection would be improved.

#### Acknowledgments

This work was supported by Grants-in-Aid for Scientific Research A (22H00309), Scientific Research B (21H03733, 21H03736, and 22H03872), Exploratory Research (22K18997), and JSPS Fellows for Young Scientists (23KJ1592) from the Japan Society for the Promotion of Science. JST A-STEP, Foundation from Cooperative Research Project of the Research Center for Biomedical Engineering, Kazuchika Okura Memorial Foundation, Asahi Glass Foundation, Konica Minolta Science and Technology Foundation, and Nakatani Foundation are also acknowledged.

## References

- 1 S. E. Derenzo, M. J. Weber, E. Bourret-Courchesne, and M. K. Klintonberg: Nucl. Instrum. Methods Phys. Res., A **505** (2003) 111. [https://doi.org/10.1016/S0168-9002\(03\)01031-3](https://doi.org/10.1016/S0168-9002(03)01031-3)
- 2 W. W. Moses: Nucl. Instrum. Methods Phys. Res., Sect. A **487** (2002) 123. [https://doi.org/10.1016/S0168-9002\(02\)00955-5](https://doi.org/10.1016/S0168-9002(02)00955-5)
- 3 T. Yanagida, T. Kato, D. Nakauchi, and N. Kawaguchi: Jpn. J. Appl. Phys. **62** (2023) 010508. <https://doi.org/10.35848/1347-4065/ac9026>
- 4 P. Lecoq: Nucl. Instrum. Methods Phys. Res. A **809** (2016) 130. <https://doi.org/10.1016/j.nima.2015.08.041>
- 5 J. Glodo, Y. Wang, R. Shawgo, C. Brecher, R. H. Hawrami, J. Tower, and K. S. Shah: Phys. Procedia **90** (2017) 285. <https://doi.org/10.1016/j.phpro.2017.09.012>
- 6 K. Watanabe, T. Yanagida, K. Fukuda, A. Koike, T. Aoki, and A. Uritani: Sens. Mater. **27** (2015) 1. <https://doi.org/10.18494/SAM.2015.1093>
- 7 C. L. Melcher, J. S. Schweitzer, R. A. Manente, and C. A. Peterson: J. Cryst. Growth **109** (1991) 37. [https://doi.org/10.1016/0022-0248\(91\)90155-X](https://doi.org/10.1016/0022-0248(91)90155-X)
- 8 D. Shiratori, H. Fukushima, D. Nakauchi, T. Kato, N. Kawaguchi, and T. Yanagida: Sens. Mater. **35** (2023) 439. <https://doi.org/10.18494/SAM4140>
- 9 H. Fukushima, D. Nakauchi, T. Kato, N. Kawaguchi, and T. Yanagida: Jpn. J. Appl. Phys. **62** (2023) 010506. <https://doi.org/10.35848/1347-4065/ac9105>
- 10 Y. Zorenko, V. Gorbenko, I. Konstankevych, B. Grinev, and M. Globus: Nucl. Instrum. Methods Phys. Res., Sect. A **486** (2002) 309. [https://doi.org/10.1016/S0168-9002\(02\)00725-8](https://doi.org/10.1016/S0168-9002(02)00725-8)
- 11 K. Okazaki, D. Onoda, D. Nakauchi, N. Kawano, H. Fukushima, T. Kato, N. Kawaguchi, and T. Yanagida: Sens. Mater. **34** (2022) 575. <https://doi.org/10.18494/SAM3678>
- 12 T. Yanagida, H. Takahashi, T. Ito, D. Kasama, T. Enoto, M. Sato, S. Hirakuri, M. Kokubun, K. Makishima, T. Yanagitani, H. Yagi, T. Shigeta, and T. Ito: IEEE Trans. Nucl. Sci. **52** (2005) 1836. <https://doi.org/10.1109/TNS.2005.856757>
- 13 S. Liu, J. A. Mares, X. Feng, A. Vedda, M. Fasoli, Y. Shi, H. Kou, A. Beitlerova, L. Wu, C. D'Ambrosio, Y. Pan, and M. Nikl: Adv. Opt. Mater. **4** (2016) 731. <https://doi.org/10.1002/adom.201500691>
- 14 T. Kunikata, T. Kato, D. Shiratori, P. Kantuptim, D. Nakauchi, N. Kawaguchi, and T. Yanagida: Sens. Mater. **35** (2023) 491. <https://doi.org/10.18494/SAM4145>
- 15 M. Koshimizu: Jpn. J. Appl. Phys. **62** (2023) 010503. <https://doi.org/10.35848/1347-4065/ac94fe>
- 16 G. A. Bray: Anal. Biochem. **1** (1960) 279. [https://doi.org/10.1016/0003-2697\(60\)90025-7](https://doi.org/10.1016/0003-2697(60)90025-7)
- 17 T. Okuyama, and Y. Kobayashi: Arch. Biochem. Biophys. **95** (1961) 242. [https://doi.org/10.1016/0003-9861\(61\)90141-2](https://doi.org/10.1016/0003-9861(61)90141-2)
- 18 H. Kimura, T. Fujiwara, M. Tanaka, T. Kato, D. Nakauchi, N. Kawaguchi, and T. Yanagida: Sens. Mater. **35** (2023) 513. <https://doi.org/10.18494/SAM4146>
- 19 T. Wu, Z. Hua, G. Tang, H. Ban, H. Cai, J. Han, H. Liu, S. Liu, S. Qian, L. Qin, J. Ren, X. Sun, X. Sun, Y. Wen, and Y. Zhu: J. Am. Ceram. Soc. **106** (2023) 476. <https://doi.org/10.1111/jace.18761>
- 20 H. Masai, and T. Yanagida: Jpn. J. Appl. Phys. **62** (2023) 010606. <https://doi.org/10.35848/1347-4065/ac91b8>
- 21 N. Kiwsakunkran, N. Chanthima, H. Kim, and J. Kaewkhao: Phys. Status Solidi A **220** (2023) 1. <https://doi.org/10.1002/pssa.202200437>
- 22 Y. Takebuchi, D. Shiratori, T. Kato, D. Nakauchi, N. Kawaguchi, and T. Yanagida: Sens. Mater. **35** (2023) 507. <https://doi.org/10.18494/SAM4142>
- 23 H. Masai, H. Kimura, M. Akatsuka, T. Kato, N. Kitamura, and T. Yanagida: J. Lumin. **241** (2022) 118481. <https://doi.org/10.1016/j.jlumin.2021.118481>
- 24 T. Yanagida, J. Ueda, H. Masai, Y. Fujimoto, and S. Tanabe: J. Non-Cryst. Solids **431** (2016) 140. <https://doi.org/10.1016/j.jnoncrysol.2015.04.033>
- 25 M. E. Moore, H. Xue, P. Vilmercati, S. J. Zinkle, N. Mannella, and J. P. Hayward: J. Non-Cryst. Solids **498** (2018) 145. <https://doi.org/10.1016/j.jnoncrysol.2018.06.004>
- 26 C. W. E. van Eijk: Radiat. Meas. **38** (2004) 337. <https://doi.org/10.1016/j.radmeas.2004.02.004>
- 27 R. Wervelman, K. Abrahams, H. Postma, J. G. L. Booten, and A. G. M. Van Hees: Nucl. Phys. A **526** (1991) 265. [https://doi.org/10.1016/0375-9474\(91\)90287-G](https://doi.org/10.1016/0375-9474(91)90287-G)
- 28 R. T. Kouzes, A. T. Lintereur, and E. R. Siciliano: Nucl. Instrum. Methods Phys. Res., Sect. A **784** (2015) 172. <https://doi.org/10.1016/j.nima.2014.10.046>
- 29 W. Chuirazzi, A. Craft, B. Schillinger, S. Cool, and A. Tengattini: J. Imaging **6** (2020) 124. <https://doi.org/10.3390/jimaging6110124>

- 30 M. Katagiri, K. Sakasai, M. Matsubayashi, and T. Kojima: Nucl. Instrum. Methods Phys. Res., Sect. A **529** (2004) 317. <https://doi.org/10.1016/j.nima.2004.05.003>
- 31 S. Saha, H. J. Kim, P. Aryal, M. Tyagi, R. Barman, J. Kaewkhao, S. Kothan, and S. Kaewjaeng: Radiat. Meas. **134** (2020) 106319. <https://doi.org/10.1016/j.radmeas.2020.106319>
- 32 M. Ishii, Y. Kuwano, T. Asai, S. Asaba, M. Kawamura, N. Senguttuvan, T. Hayashi, M. Kobayashi, M. Nikl, S. Hosoya, K. Sakai, T. Adachi, T. Oku, and H. M. Shimizu: Nucl. Instrum. Methods Phys. Res., Sect. A **537** (2005) 282. <https://doi.org/10.1016/j.nima.2004.08.027>
- 33 Y. Fujimoto, T. Yanagida, S. Wakahara, S. Suzuki, S. Kurosawa, and A. Yoshikawa: Radiat. Meas. **55** (2013) 124. <https://doi.org/10.1016/j.radmeas.2013.01.017>
- 34 M. Kaburagi, K. Shimazoe, Y. Terasaka, H. Tomita, S. Yoshihashi, A. Yamazaki, A. Uritani, and H. Takahashi: Nucl. Instrum. Methods Phys. Res., Sect. A **1046** (2023) 167636. <https://doi.org/10.1016/j.nima.2022.167636>
- 35 S. A. Umar, M. K. Halimah, K. T. Chan, and A. A. Latif: J. Non-Cryst. Solids **472** (2017) 31. <https://doi.org/10.1016/j.jnoncrystol.2017.07.013>
- 36 S. S. Hajer, M. K. Halimah, A. Zakaria, and M. N. Azlan: Mater. Sci. Forum **846** (2016) 63. <https://doi.org/10.4028/www.scientific.net/MSF.846.63>
- 37 W. Rittisit, N. Wantana, A. Butburee, Y. Ruangtaweep, J. Padchagri, S. Rujirawat, P. Manyum, P. Kidkhunthod, R. Yimnirun, S. Kothan, H. J. Kim, A. Prasatkhetragarn, and J. Kaewkhao: Radiat. Phys. Chem. **185** (2021) 109498. <https://doi.org/10.1016/j.radphyschem.2021.109498>
- 38 H. H. Hegazy, M. S. Al-Buriah, F. Alresheedi, S. Alraddadi, H. Arslan, and H. Algarni: J. Inorg. Organomet. Polym. Mater. **31** (2021) 2331. <https://doi.org/10.1007/s10904-021-01933-2>
- 39 S. Stalin, A. Edukondalu, I. Boukhris, Z. A. Alrowaili, A. M. Al-Baradi, I. O. Olarinoye, D. K. Gaikwad, and M. S. Al-Buriah: Ceram. Int. **47** (2021) 30137. <https://doi.org/10.1016/j.ceramint.2021.07.192>
- 40 T. Yanagida: Opt. Mater. **35** (2013) 1987. <https://doi.org/10.1016/j.optmat.2012.11.002>
- 41 D. Nakauchi, F. Nakamura, T. Kato, N. Kawaguchi, and T. Yanagida: Sens. Mater. **35** (2023) 467. <https://doi.org/10.18494/SAM4138>
- 42 K. Okazaki, D. Nakauchi, H. Fukushima, T. Kato, N. Kawaguchi, and T. Yanagida: Appl. Sci. **12** (2022) 11624. <https://doi.org/10.3390/app122211624>
- 43 O. A. Lopez, J. McKittrick, and L. E. Shea: J. Lumin. **71** (1997) 1. [https://doi.org/10.1016/S0022-2313\(96\)00123-8](https://doi.org/10.1016/S0022-2313(96)00123-8)
- 44 M. Shang, D. Geng, X. Kang, D. Yang, Y. Zhang, and J. Lin: Inorg. Chem. **51** (2012) 11106. <https://doi.org/10.1021/ic301662c>
- 45 S. D. Jackson: Nat. Photonics **6** (2012) 423. <https://doi.org/10.1038/nphoton.2012.149>
- 46 N. Kawano, D. Nakauchi, K. Fukuda, G. Okada, N. Kawaguchi, and T. Yanagida: Jpn. J. Appl. Phys. **57** (2018) 102401. <https://doi.org/10.7567/JJAP.57.102401>
- 47 P. Kantuptim, D. Nakauchi, T. Kato, N. Kawaguchi, and T. Yanagida: Sens. Mater. **34** (2022) 603. <https://doi.org/10.18494/SAM3690>
- 48 Y. Fujimoto, M. Sugiyama, T. Yanagida, S. Wakahara, S. Suzuki, S. Kurosawa, V. Chani, and A. Yoshikawa: Opt. Mater. **35** (2013) 2023. <https://doi.org/10.1016/j.optmat.2012.10.010>
- 49 K. Okazaki, D. Nakauchi, H. Fukushima, T. Kato, N. Kawaguchi, and T. Yanagida: Sens. Mater. **35** (2023) 459. <https://doi.org/10.18494/SAM4144>
- 50 T. Yanagida, K. Kamada, Y. Fujimoto, H. Yagi, and T. Yanagitani: Opt. Mater. **35** (2013) 2480. <https://doi.org/10.1016/j.optmat.2013.07.002>
- 51 T. Yanagida, Y. Fujimoto, T. Ito, K. Uchiyama, and K. Mori: Appl. Phys. Express **7** (2014) 062401. <https://doi.org/10.7567/APEX.7.062401>
- 52 X. Wang, F. Lou, S. Wang, C. Yu, D. Chen, and L. Hu: Opt. Mater. **42** (2015) 287. <https://doi.org/10.1016/j.optmat.2015.01.014>
- 53 I. I. Kindrat, B. V. Padlyak, R. Lisiecki, and V. T. Adamiv: J. Non-Cryst. Solids **521** (2019) 119477. <https://doi.org/10.1016/j.jnoncrystol.2019.119477>
- 54 R. Kibar, A. Çetin, Y. Tuncer, S. Uysal, P. D. Townsend, A. Canimoglu, T. Karali, and N. Can: Phys. Procedia **2** (2009) 379. <https://doi.org/10.1016/j.phpro.2009.07.023>
- 55 Y. T. Arslanlar, Z. Kotan, R. Kibar, A. Canimoglu, and N. Can: Spectrosc. Lett. **46** (2013) 590. <https://doi.org/10.1080/00387010.2013.771370>
- 56 T. Kato, D. Nakauchi, N. Kawaguchi, and T. Yanagida: Opt. Mater. **106** (2020) 110028. <https://doi.org/10.1016/j.optmat.2020.110028>
- 57 D. Totsuka, T. Yanagida, M. Sugiyama, J. Pejchal, Y. Fujimoto, Y. Yokota, and A. Yoshikawa: Opt. Mater. **34** (2012) 627. <https://doi.org/10.1016/j.optmat.2011.09.008>

- 58 H. Fukushima, D. Nakauchi, T. Kato, N. Kawaguchi, and T. Yanagida: *Radiat. Meas.* **133** (2020) 106280. <https://doi.org/10.1016/j.radmeas.2020.106280>
- 59 P. Kantuptim, M. Akatsuka, D. Nakauchi, T. Kato, N. Kawaguchi, and T. Yanagida: *J. Alloys Compd.* **847** (2020) 156542. <https://doi.org/10.1016/j.jallcom.2020.156542>
- 60 T. Yanagida: *Proc. Jpn. Acad. Ser. B* **94** (2018) 75. <https://doi.org/10.2183/pjab.94.007>
- 61 D. J. Robbins: *J. Electrochem. Soc.* **127** (1980) 2694. <https://doi.org/10.1149/1.2129574>
- 62 M. Seshadri, M. Radha, H. Darabian, L. C. Barbosa, M. J. V. Bell, and V. Anjos: *J. Therm. Anal. Calorim.* **138** (2019) 2971. <https://doi.org/10.1007/s10973-019-08344-z>